Technical University of Denmark

DTU

SAR antenna design for ambiguity and multipath suppression

Christensen, Erik Lintz; Dich, Mikael

Published in:
International Geoscience and Remote Sensing Symposium

Link to article, DOI:
10.1109/IGARSS.1993.322219

Publication date:
1993

Document Version
Publisher's PDF, also known as Version of record

[Link back to DTU Orbit](#)

DTU Library
Technical Information Center of Denmark

SAR ANTENNA DESIGN FOR AMBIGUITY AND MULTIPATH SUPPRESSION

Erik Lintz Christensen and Mikael Dich

Electromagnetics Institute, Technical University of Denmark
B-348, Lundtoftevej 100, DK-2800 Lyngby, Denmark; Fax +45 45 93 16 34

ABSTRACT

A high resolution airborne Synthetic Aperture Radar (SAR) has been developed at Electromagnetics Institute (EMI) for remote sensing applications. This paper considers the radiation of antennas for a SAR system from a systems perspective. The basic specifications of an idealised antenna are obtained from the required swath and the azimuth footprint needed for the SAR processing. The radiation from a real antenna causes unwanted signal returns that lead to intensity variations (multipath) and ghost echoes (ambiguity). Additional specifications are deduced by considering these signals. The requirements are illustrated by examples from a realised dual polarised antenna for a C-band SAR.

INTRODUCTION

Antennas for airborne strip-mapping Synthetic Aperture Radar (SAR) applications have to fulfil requirements on radiation pattern, polarisation purity, return loss, and power handling capability. The present paper considers some of the requirements to the radiation pattern. The remaining requirements have been studied in previous documentation [1..7] but with less focus on the requirements arising from the radiation outside the required main beam.

The antenna radiation pattern must be adapted to suit a compromise between conflicting requirements: A high antenna gain with a sharp pattern specification is preferable but the space for the antenna installation on an aircraft is limited, especially when the antenna is stabilised against roll, pitch and yaw.

The minimum width of the main lobe of the radiation pattern in azimuth (i.e., in the direction of flight) is determined by the required resolution. The resolution in the azimuth direction is obtained using the Doppler shift caused by the movement of the aircraft. To obtain a high resolution a wide main lobe is required. Since the Doppler spectrum is obtained using the radar pulses, the measured Doppler spectrum is a sampled version of the true spectrum. Thus the antenna must suppress signals that could cause aliasing in the Doppler frequency spectrum, which in turn causes azimuth ambiguity, i.e.:

- The radiation outside the necessary main lobe in azimuth must be sufficiently low to keep the azimuth ambiguity at a low level.

The radiation pattern in elevation (i.e., in the vertical plane perpendicular to the flight plane) must assure a reasonably even illumination of the area to be mapped. In addition the antenna must have low radiation in two directions:

- In the direction of the opposite side of the aircraft. Due to the nature of the SAR system, signal returns from the opposite side of the aircraft cannot be separated from the returns from the mapped area. Thus radiation in this direction causes left/right ambiguity.

- In the direction towards the wing. Radiation from the antenna in this direction can cause multipath interference and ambiguity in both range and azimuth.

The specific requirements discussed in the present paper are deduced from EMI's SAR. The SAR system employs antenna stabilisation on three axes. Thus it is possible to point the antenna accurately at the strip to be mapped and perpendicular to the desired ground track virtually independent of the aircraft motion.

Similarly, the radar pulse repetition frequency is locked to the ground velocity. Thus the transmitter emits pulses each time the aircraft has moved a specific distance along the track.

AZIMUTH RADIATION PATTERN

Doppler shift: The Doppler shift is zero for echoes from targets lying in a plane perpendicular to the flight track. Echoes with positive Doppler shift are obtained from targets ahead of the aircraft and echoes with negative Doppler shift are obtained from targets behind. The Doppler shift history is used in the SAR processing to obtain the azimuth resolution.
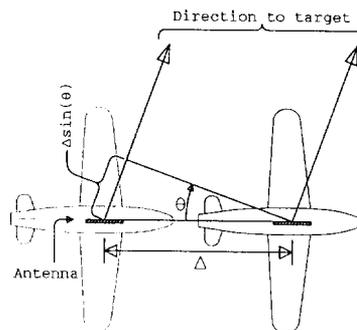

Fig. 1: SAR geometry in the horizontal plane

With the geometry as show in figure 1, the Doppler phase shift φ_D is given by:

$$\varphi_D = 4\pi \frac{\Delta}{\lambda} \sin(\theta) \tag{1}$$

where θ represents the off axis angle to the target and Δ represents the displacement of the antenna along the flight track.

To achieve an azimuth resolution of Δr we must at least have an antenna pattern wide enough to get information (i.e., signal return) from an angular sector determined by:

$$\frac{-\lambda}{4\Delta r} \leq \sin(\theta) \leq \frac{+\lambda}{4\Delta r} \tag{2}$$

The phase shift versus displacement results in a Doppler spectrum when the aircraft moves with constant velocity. For the SAR in question the Doppler spectrum is sampled at fixed aircraft displacements Δs. An undesired consequence of sampling is that various parts of the Doppler spectrum are transferred to overlap the desired spectrum. This fact causes targets ahead of and behind the aircraft to be imaged on top of the targets on axis unless the antenna suppresses radiation in the harmful directions. The direction θ_s from which the Doppler frequency equals the sampling frequency is given by:

$$\sin(\theta_s) = \frac{\lambda}{2\Delta s} \qquad (3)$$

where Δs is the distance of flight between two consecutive radar pulses.

Azimuth pattern: From the above we can deduce the following characteristics of the azimuth pattern of the antenna:

First the pattern has a main lobe around $\theta = 0$. This is the angular sector for the azimuth radiation pattern that is needed to obtain the required resolution. The symmetrical range is given by (2).

Second the azimuth radiation pattern must suppress radiation in angular sectors of a size as given by (2) but centred around $\sin(\theta) = \pm p \sin(\theta_s)$, p integer ≠ 0 (the aliasing bands), since returned signals from these directions will be transferred to overlap the desired band of the Doppler spectrum.

Third we have the angular sectors in between. The radiation here is uncritical, since signals in these sectors can be removed by filtering after the sampling.

In figure 2 an outline of the azimuth radiation pattern is shown with the aliasing bands indicated.
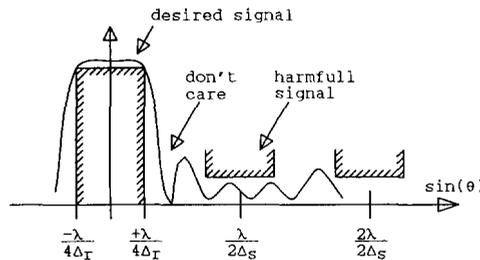

Fig. 2: Outline of azimuth radiation pattern

AZIMUTH AMBIGUITY

It is not possible to realise a perfect azimuth pattern with an antenna of finite extends. To describe the performance of the antenna we introduce the two-way ambiguous integrated sidelobe ratio (ISLR) defined as:

$$ISLR = \frac{\displaystyle\sum_i \int_{u=\frac{i\lambda}{2\Delta s}-\frac{\lambda}{4\Delta_r}}^{u=\frac{i\lambda}{2\Delta s}+\frac{\lambda}{4\Delta_r}} (E(u)\cdot E(u)^*)^2\,du}{\displaystyle\int_{u=\frac{-\lambda}{4\Delta_r}}^{\frac{\lambda}{4\Delta_r}} (E(u)\cdot E(u)^*)^2\,du} \qquad (4)$$

$$\left(-\frac{2\Delta_s}{\lambda} \le i \le \frac{2\Delta_s}{\lambda}\right) \wedge (i \ne 0) \ ; \ u = \sin(\theta)$$

In (4) E is the amplitude of the pattern. The denominator represents the integrated signal power in the processed part of the radiation pattern. The numerator represents the total integrated signal power in all the aliasing bands. Equation (4) takes advantage of the fact that although the data in the aliasing bands will all focus, they contribute with images from different parts of the scene. Thus these data will not correlate with the true image or with each other.

The radiation pattern of a real antenna is more or less frequency dependent and the bandwidth of the transmitted signal must be taken into account. The ISLR must be calculated as an average over the exploited frequency range.

The design goal for the azimuth ambiguity for EMI's SAR is -30 dB measured as the total of all ambiguous targets. In addition to the aliasing bands in the azimuth sidelobes, two additional sources could contribute to the azimuth ambiguity: a less than ideal filtering of the "don't care" bands and reflections in the wing. The last source is a consequence of the pitch of the wing and will be discussed in the elevation section. If we assign equal shares to each of the three sources we get:

$$ISLR < \frac{1}{3\cdot 1000} \sim -34.8 \text{ dB} \qquad (5)$$

The ISLR for a specific antenna depends on the selected resolution. We will consider the two resolutions Δr = 0.5 m and Δr = 1.5 m and a sampling spacing in azimuth of 0.375 m.

ANTENNA EXAMPLES

The antenna for EMI's SAR is built using microstrip technology. The antenna is manufactured by 4 identical panels as shown in figure 3. It has a total size of 1.35 x 0.35 m and is designed for the frequency band 5.3 GHz ± 50 MHz. Each panel has 7 square microstrip patches in the elevation direction and 8 patches in the azimuth direction. The 8 columns of patches on each panel have equal excitation. It has been verified that the radiation pattern in azimuth and elevation are virtually independent of each other. Thus we can use (4) for the calculation of ISLR, independent of the elevation angle. The pattern of the total antenna can be modified somewhat by changing the excitation of the 4 individual panels.
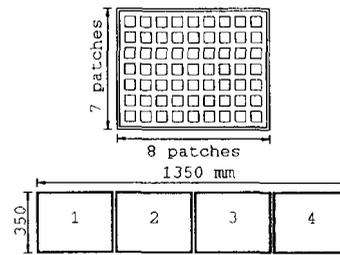

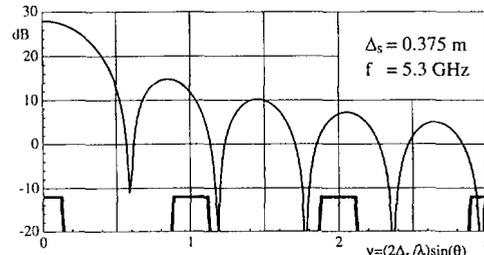Fig. 3: Microstrip antenna for 5.3 GHz SAR

Fig. 4: Processed band and aliasing bands; resolution 1.5 m.

First we examine the radiation from the antenna, when the four panels have with equal excitations. The radiation of the antenna with processed signal band and aliasing bands is shown in figure 4 (resolution Δr = 1.5 m) and figure 5 (resolution Δr = 0.5 m), as a function of the normalised Doppler shift. It can be seen directly from figure 4 that a smaller Δs could move the aliasing bands to be centred at the nulls of the pattern but that would increase the data rate of the SAR.
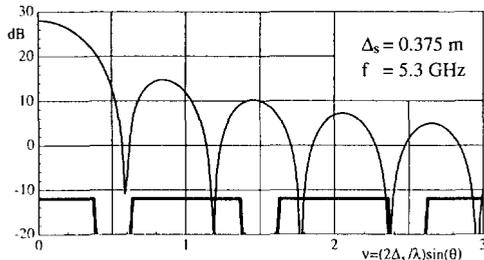
Fig. 5: Processed band and aliasing bands; resolution 0.5 m.

Calculations of the ISLR and antenna gain for the two cases give:

Resolution:	ISLR	Gain
1.5 m	-27.3 dB	28.3 dB
0.5 m	-25.7 dB	-

Second we alter the excitation of the two outermost panels, relative to the excitation of the innermost. The ISLR proves to have a minimum for the excitations 0.6, 1.0, 1.0, 0.6 of the four panels. The corresponding radiation patterns with aliasing bands are shown in figure 6 (resolution Δr = 1.5 m) and figure 7 (resolution Δr = 0.5 m).

New calculations of the ISLR and antenna gain for the two cases give:

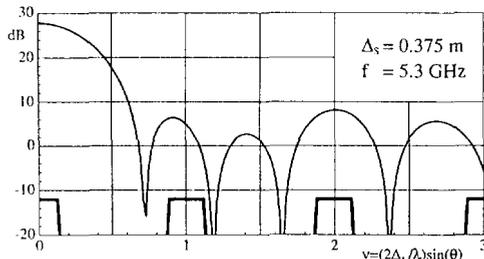| Resolution:	ISLR	Gain
1.5 m	-36.2 dB	27.9 dB
0.5 m	-35.7 dB	-

Fig. 6: Azimuth pattern for minimum ambiguity;
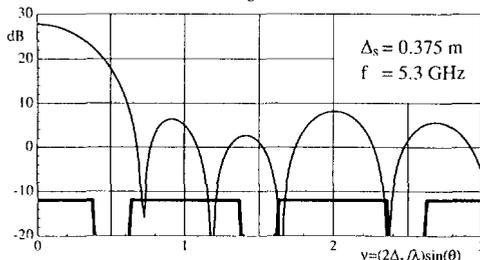Processed band and aliasing bands for resolution 1.5 m.

Fig. 7: Azimuth pattern for minimum ambiguity;
Processed band and aliasing bands for resolution 0.5 m.

As can be seen, the ISLR has been reduced considerably at the cost of a slight reduction of the antenna gain, i.e., a slightly degraded system sensitivity.

The examples given above clearly show that azimuth ambiguity can be reduced by proper design of the antenna even when the manufacturing requirements limit the degree of freedom to the excitation of the four individual antenna panels.

ELEVATION RADIATION PATTERN:

The antenna of EMI's SAR is mounted in a pod under the hull of the aircraft next to the wing. Thus the wing acts as a mirror with limited width and a slight curvature.

The magnitude of the reflection is difficult to evaluate accurately. The wing reflections will be smaller than the reflections from an ideal mirror partly because the wing is of limited extend and partly because the wing is curved which make the reflected signal to diverge slightly. A plane, infinite, mirror will be a prudent approximation.

Multipath: The wing causes multipath propagation which gives more echoes with different delays from a single target. The effect of the wing is equivalent to adding a mirror antenna that will have the main beam pointing upwards when the real antenna main beam is pointing downwards.
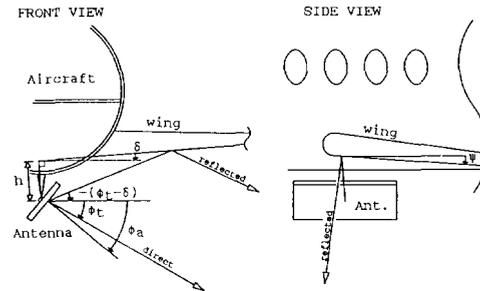
Fig. 8: Antenna and wing reflection geometry.

In figure 8 the geometry of the antenna and the wing is shown. The height h denotes the distance between the antenna centre and the plane of the wing. ϕ_t denotes the depression angle to the target, ϕ_a denotes the depression angle of the antenna maximum, and δ is the across track tilt of the wing. Aircraft roll will cause δ to change.

The additional delay of a reflected echo is less than the range resolution for the actual installation. Thus the reflected echoes cause smearing rather than ambiguous echoes in range. In addition a periodic amplitude variation is imposed on the radar image in range, since the phase of the echoes reflected in the wing will vary relative to the direct echo with ϕ_t and δ.

The combined elevation pattern will have ripples due to the interfering sidelobe from the image antenna. The ratio of the power in the sidelobe of the image antenna versus the power in the main lobe of the real antenna radiated in the direction of the target will be:

$$R_W = \frac{G(-\phi_t + 2\delta - \phi_a)}{G(\phi_t - \phi_a)} \qquad (6)$$

where G is the power gain of the antenna as a function of the angle in elevation from the peak gain.

The requirement to the ratio between maximum and minimum of the signal level is set to 0.5 dB peak-peak. Since the signal passes the antenna twice the requirement to the ripples

-786-

on the radiation pattern will be 0.25 dB peak-peak. This leads to:

$$R_W \leq \left(\frac{10^{0.25/20} - 1}{10^{0.25/20} + 1} \right)^2 \sim -36.8 \text{ dB} \qquad (7)$$

Provided the wing is without pitch we get from (7) the following relation in the elevation plane between the antenna gain in the direction of the wing and the gain in the direction of the target:

$$10\log(G(-\phi_t + 2\delta - \phi_a)) \leq 10\log(G(\phi_t - \phi_a)) - 36.8 \text{ dB} \quad (8)$$

Wing pitch: For the aircraft on which EMI's SAR is mounted the wing has a pitch, ψ, (tilt along track) around 4°. This will cause the reflected signals to turn forward with an angle of 2ψ or around 8°.

The pitch of the antenna implies that the true (combined) pattern is the sum of the antenna pattern and the mirror antenna pattern, the latter being shifted 8° in azimuth. The normalised angular parameter v used for the antenna patterns is for 8°:

$$v = \frac{2\Delta s}{\lambda} \sin(\theta) = 1.844 \qquad (9)$$

As can be observed on the azimuth patterns, the sidelobes near $v = 1.844$ are below 17 dB.

The elevation sidelobe interfering with the main lobe is thus reduced further by the azimuth pattern. This leads to a relaxed requirement on the sidelobes of the elevation pattern in the direction of the wing to be 17 dB below the requirement stated in (8), i.e.:

$$10\log(G(-\phi_t + 2\delta - \phi_a)) \leq 10\log(G(\phi_t - \phi_a)) - 19.8 \text{ dB} \quad (10)$$

More azimuth ambiguity: The main beam of the mirror antenna is pointing forward and could (dependent on the wing pitch and the width of the main lobe) contribute to the signal in the aliasing bands and will then increase the azimuth ambiguity. This is the situation for the antenna in question and that fact leads to an additional constraint to the elevation pattern.

The mirrored main lobe gives one significant contribution to the azimuth ambiguity that must be below -34.8 dB (5). It is assumed in (5) that the three mentioned sources contribute equally to the azimuth ambiguity power. However, the signal from the main lobe of the mirror antenna will add coherently to the signal from one of the sidelobes of the real antenna.

The combined radiation pattern cannot be calculated since the aircraft pitch is variable. It can be shown that the signal in the mirrored main lobe must be 7.6 dB below the -34.8 dB in order to be certain that the mirrored main lobe does not cause an increase of the azimuth ambiguity by more than specified in (5). A safe requirement to the elevation pattern will then be a suppression of (34.8+7.6)/2 dB where the division by two comes from the two-way action of the antenna. This leads to the following requirement to the elevation pattern:

$$10\log(G(-\phi_t + 2\delta - \phi_a)) \leq 10\log(G(\phi_t - \phi_a)) - 21.2 \text{ dB} \quad (11)$$

Equation (11) becomes the final constrain on the elevation pattern in the direction of the wing, since (11) imposes a tighter requirement than (10).

Left/right ambiguity: The specification of the left/right ambiguity imposes constrains on the other side of the elevation pattern. If we require the ambiguous signal coming from the opposite side of the aircraft to be suppressed 40 dB we get:

$$10\log(G(180° - \phi_t - \phi_a)) \leq 10\log(G(\phi_t - \phi_a)) - 20.0 \text{ dB} \quad (12)$$

Main lobe: Finally, it is preferred that the radar echoes are fairly independent of the range and thus the elevation angle. This leads to an elevation profile equal to the well-known modified cosecant squared pattern. This profile is difficult to

obtain accurately, since real antennas are of limited extend (e.g., seven patches for EMI's SAR antenna in the vertical direction). Correction for the difference between the ideal and the real elevation profile can be made to some extent using Sensitivity Time Control (STC) in the receiver. When accurately calibrated signals are required it is more important that the elevation profile is a smooth curve without ripples.

ANTENNA EXAMPLE:

The calculated radiation pattern in elevation is shown in figure 9 for the actual antenna. Equations (11) and (12) can the be used to determine the permitted range of the parameters, i.e., the depression angle to the target (ϕ_t) and the depression angle of the antenna maximum (ϕ_a), when the range for the tilt of the wing across track (δ) is estimated.
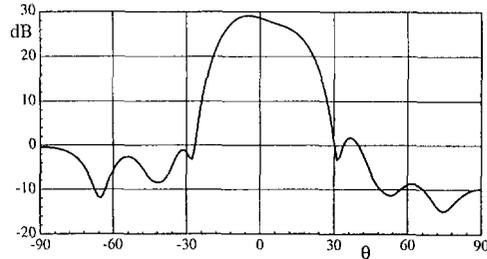

Fig. 9: Antenna pattern in elevation

CONCLUSION:

The specification for the azimuth- and elevation radiation pattern have been derived for a SAR antenna. The azimuth ambiguity and problems caused by reflections in the aircraft wing have been studied in details. Examples of calculated radiation patterns for a real SAR antenna, consisting of microstrip patches, have been given.

REFERENCES

[1] S. Nørvang Madsen, N. Skou and E. Lintz Christensen
A New C-band SAR for ERS-1 underflights
Radar-90, IEEE Radar conference in Arlington, VA, May 7-10, 1990, pp 223-227

[2] Frederik Tuxen and Mikael Dich
Calibration of SAR Antenna by Spherical Near-Field Measurements
R 457, Electromagnetics Institute, Technical University of Denmark, Lyngby, Denmark, Feb. 1991

[3] Mikael Dich
Slotted Waveguide Array Antenna for Synthetic Aperture Radar
R 471, Electromagnetics Institute, Technical University of Denmark, Lyngby, Denmark, May 1991

[4] S. Nørvang Madsen, E. Lintz Christensen, N. Skou, and J. Dall
The Danish SAR System; Design and Initial Tests
IEEE Transactions on Geoscience and Remote Sensing, Vol 29, No 3, May 1991, pp 417-426.

[5] Kim Woelders and Johan Granholm
Design and Performance of a Dual-Linearly Polarized C-band Microstrip Array Antenna
Accepted for "Second International Workshop on Radar Polarimetry" (Nantes, France, September 1992).

[6] R.W. Bayma and P.A. McInnes
Aperture Size and Ambiguity Constraints for a Synthetic Aperture Radar
IEEE International Radar Conference, Arlington, VA., 1975, pp 499-504

[7] Fuk-Kwok Li and W.T.K. Johnson
Ambiguities in Spaceborne Synthetic Aperture Radar Systems
IEEE Transactions on Aerospace and Electronic Systems, Vol. AES-19, No. 3, May 1983, pp. 389-397